Severity parameter and global importance factor of Non-Newtonian models in 3D reconstructed human Left Coronary Artery

Johannes V. SOULIS[*], Kypriani V. SERALIDOU[1], Yiannis S. CHATZIZISIS[2], George D. GIANNOGLOU[2]

* Corresponding author: Tel: ++302310994837; Fax: ++302310994837; Email: jvsoulis@med.auth.gr
1: Fluid Mechanics, Demokrition University of Thrace, Greece
2: Cardiovascular Engineering and Atherosclerosis Laboratory,
1st Cardiology Department, Aristotle University of Thessaloniki, Greece

Abstract The capabilities and limitations of various molecular viscosity models, when testing Left Coronary Artery (LCA) tree, were analyzed via: molecular viscosity, local and global non-Newtonian importance factors, Wall Shear Stress (*WSS*) and Wall Shear Stress Gradient (*WSSG*). Seven non-Newtonian molecular viscosity models, plus the Newtonian one, were compared. Dense grid of 620000 nodes located, mostly, at near to low *WSS* flow regions (endothelium regions) is needed for current LCA application. The *WSS* distribution yields a consistent LCA pattern for nearly all non-Newtonian models. High molecular viscosity, low *WSS* low *WSSG* values appear at proximal LCA regions at the outer walls of the major bifurcation. The global importance factor for the non-Newtonian power law model yields 76.7% (non-Newtonian flow), while for the Generalized power law model this value is 6.1% (Newtonian flow). The capabilities of the applied non-Newtonian law models appear at low strain rates. The Newtonian blood flow treatment is considered to be a good approximation at mid-and high-strain rates. In general, the non-Newtonian power law and the Generalized power law blood viscosity models are considered to approximate the molecular viscosity and *WSS* calculations in a more satisfactory way.
.

Keywords: Non-Newtonian Blood Flow, Importance Factor, Severity Parameter, Coronary Artery

1. Introduction

The choice and application of an appropriate non-Newtonian model for blood flow analysis is crucial in achieving acceptable results. The role of viscosity in the development and progression of coronary heart disease is important (Becker, 1993; Cho, et al., 1991). Atherosclerosis shows preference at sites where flow is either slow or disturbed and where Wall Shear Stress (*WSS*) as well as their gradients are low (Farmakis et al., 2004). A hypothesis, that an increased plasma viscosity may be a link between cardiovascular risk factors and coronary heart disease, is supported (Junker et al. 1998). According to non-Newtonian behavior, viscosity is velocity gradient-dependent and subsequently varies along the course of the vessel. Henceforth, the variation is dependent on the applied flow conditions, vascular geometry, flow particularities and local flow composition. However, little research has focused on the exact role of local viscosity differentiation within the coronary artery tree and its implications to atherogenesis.

In the early Computational Fluid Dynamics work in the cardiovascular system, the blood was treated as a Newtonian fluid. In the last few years, a number of papers have been published dealing with molecular viscosity (Soulis, et al., 2006) as well as with the Wall Shear Stress Gradient (*WSSG*), (Farmakis et al., 2004) distribution treating the flow as a non-Newtonian fluid (Giannoglou et al., 2005). Most of these research was concentrated on particular regions of the coronary trees.

Non-Newtonian flow comparison models in human Right Coronary Arteries (RCA) was reported (Johnston et al., 2004). Bifurcation regions of the LCA tree are of paramount hemodynamic importance, since adjacent and

opposed to the flow divider areas, where low strain rates occur, are well known sites prone to atherosclerosis. Capable blood viscosity models are needed to capture the main flow characteristics at low strain rates (Ghista et al., 1979). It is in these regions that high gradients of strain rates also occur. Many non-Newtonian models exist, but none of them is universally accepted. In the current research work, seven non-Newtonian models plus the Newtonian one are compared in a real human LCA tree. These models are: Newtonian, Carreau (Cho, et al., 1991), Modified Cross Law (Carreau-Yasuda) (Abraham et al., 2005), Power Law (Sharma et al., 1992), Non-Newtonian Power Law (Sharma et al., 1992), Generalized Power Law (Ballyk et al., 1994), Casson (Fung et al., 1993), Walburn-Schneck Law (Walburn et al., 1976). The IVUS data are derived from a particular patient. The LCA tree includes the Left Main Coronary Artery (LMCA), the Left Anterior Descending (LAD) and the Left Circumflex Artery (LCxA). The tested vessel exposes a normal, non-stenotic, geometry throughout with highly concave region present at the outer wall of the LMCA vessel just upstream to the flow divider.

2. Methods

2.1 Geometry and flow equations

The applied reconstruction method has been described in details elsewhere (Coskun et al., 2003). The IVUS catheter was inserted into the coronary artery. A biplane coronary angiogram was recorded having the catheter located at its most distal position. From each angiographic projection, a single end-diastolic frame was selected corresponding to the peak of R-wave on ECG. The resulted 2D b-spline curves were vertically extracted to the corresponding angiographic planes and intersected creating a 3D curve that corresponded to the geometrically correct 3D IVUS catheter path. All couples of contours (luminal and media-adventitia) were assigned equidistantly at the 3D reconstructed catheter path. Finally, the correctly orientated luminal contours were interpolated with additional intermediate contours, generating a 3D luminal volume. With the above mentioned approach the LCA and LCxA lumens were reconstructed separately and afterwards they merged manually according to their real geometrical configuration in humans.

The velocity is assumed to be uniform at the orifice of LMCA. The applied inflow conditions mimic typical coronary resting flow velocity of 0.17 m/s. Flow discharges were set analogous to the third power of the branching vessel diameter according to Murray's law (Murray, 1926). The numerical code solves the governing Navier-Stokes flow equations. The assumptions made about the nature of the flow are that it is 3D, steady, laminar, with no external forces applied on it, while the arterial wall is comprised from non-elastic and impermeable material. Convergence was achieved when all mass, velocity component and energy changes, from iteration to iteration, were less than 10^{-8}.

2.2 Non-Newtonian models

In total, seven different non-Newtonian computational analyses are performed using the blood viscosity models (plus the Newtonian model),

Newtonian model

$\mu = 0.00345\,Pas$

Carreau model

$$\mu = \mu_\infty + (\mu_0 - \mu_\infty)\left[1 + (\lambda\dot{\gamma})^2\right]^{(n-1)/2}$$

$\lambda = 3.313\,s$, $n = 0.3568$, $\mu_0 = 0.056\,Pa\,s$, $\mu_\infty = 0.00345\,Pa\,s$ and $\dot{\gamma}$ is the strain rate

Modified Cross Law model (Carreau-Yasuda model)

$$\mu = \mu_\infty + \frac{\mu_0 - \mu_\infty}{\left[1 + (\lambda\dot{\gamma})^b\right]^a}$$

$\mu_0 = 0.16\,Pa\,s$, $\mu_\infty = 0.0035\,Pa\,s$, $\lambda = 8.2\,sec$, $a = 1.23$ and $b = 0.64$

Power Law model

$\mu = \mu_0(\dot{\gamma})^{n-1}$, $\mu_0 = 0.035$ and $n = 0.6$

Non-Newtonian Power Law model

According to this law the fluid shear stress, denoted by τ (N/m^2), is calculated as,

$$\tau = [\eta(\dot{S})]\dot{S} \qquad \eta(\dot{S}) = k e^{\frac{T_o}{T}} \dot{S}^{n-1}$$

$$\dot{S} = \frac{\partial u_i}{\partial x_j} + \frac{\partial u_j}{\partial x_i}$$

k = consistency index ($kg - s^{n-2}/m$),

n = power-law index, T_0 = reference temperature (k), $n = 0.7$, $T_0 = 310\ k$,

$k = 0.01691\ kg - s^{n-2}/m$

Generalized Power Law model

$\mu = \lambda|\dot{\gamma}|^{n-1}$ (Units in Poise: 1.0 Poise=0.1 Pa s)

$$\lambda(\dot{\gamma}) = \mu_\infty + \Delta\mu\, exp\left[-\left(1 + \frac{|\dot{\gamma}|}{\alpha}\right) exp\left(\frac{-b}{|\dot{\gamma}|}\right)\right]$$

$$n(\dot{\gamma}) = n_\infty - \Delta n\, exp\left[-\left(1 + \frac{|\dot{\gamma}|}{c}\right) exp\left(\frac{-d}{|\dot{\gamma}|}\right)\right]$$

$\mu_\infty = 0.035$, $n_\infty = 1.0$, $\Delta\mu = 0.25$, $\Delta n = 0.45$, $a = 50$, $b = 3$, $c = 50$ and $d = 4$

Casson model

$$\mu = \left[\left(\eta^2 J_2\right)^{1/4} + 2^{-1/2}\tau_y^{1/2}\right]^2 J_2^{-1/2}$$

$|\dot{\gamma}| = 2\sqrt{J_2}$, $\tau_y = 0.1(0.625H)^3$

$\eta = \eta_0(1-H)^{-2.5}$, $\eta_0 = 0.0012\,Pa\,s$

and $H = 0.37$

Walburn-Schneck Law model

$$\mu = C_1 e^{H C_2}\left[e^{C_4(TPMA)/H^2)}\right](\dot{\gamma})^{-C_3 H}$$

(Units in Poise)

$C_1 = 0.00797$, $C_2 = 0.0608$,

$C_3 = 0.00499$, $C_4 = 14.585\ l/gr$, $H = 40$

and $TPMA = 25.9\ g/l$

2.3 Calculated variables

The Local non-Newtonian Importance factor (I_L) is defined (Johnston et al., 2004) as,

$$I_L = \frac{\mu}{\mu_\infty} \qquad (1)$$

μ_∞ equals 0.00345 (kg/m-s) and represents the undisturbed value of the dynamic blood viscosity. The distribution of this factor over the LCA clearly shows the non-Newtonian flow patches.

The averaged Global non-Newtonian importance factor *(I_G)* is defined (Ballyk et al., 1994), as,

$$I_G = \frac{1}{N}\frac{\left[\sum_{i=1}^{\substack{total\\grid\ nodes}} (\mu - \mu_\infty)^2\right]^{1/2}}{\mu_\infty}\ x\ 100 \qquad (2)$$

i is the grid node index and incorporates the cells on all LCA walls, *N* is the total grid nodes. The importance factor I_G is evaluated at each node on the surface of the artery. The I_G expresses the relative difference from the Newtonian value, in percentage terms, of each value of molecular viscosity. I_G value greater of 25.0% indicates non-Newtonian flow. At high strain rates the μ approaches the 0.00345 kg/m-s value.

The *Area Averaged WSS* (N/m^2), is defined as,

$$Area\ Averaged WSS = \frac{1}{A_o}\sum_{i=1}^{\substack{total\\cells}} |WSS|_i\ a_i \qquad (3)$$

i is the cell index on all LCA walls, a_i is the cell area, and A_o is the total surface area (=10.865 cm^2) of the tested LCA. It is utilized to measure the degree of *WSS* variation along the surfaces of the LCA .

The local magnitude of the *WSSG* (N/m^3) is defined (Farmakis et al., 2004) as,

$$WSSG = \sqrt{\left(\frac{\partial \tau_w}{\partial x}\right)^2 + \left(\frac{\partial \tau_w}{\partial y}\right)^2 + \left(\frac{\partial \tau_w}{\partial z}\right)^2} \qquad (4)$$

The components of the *WSSG* possibly have different effects upon endothelial cells. Some components, mainly those being diagonal, generate intercellular tension while the off-diagonal components possibly contribute to intercellular shearing forces (Lei et el., 2001).

The Severity Parameter (*SP*, N/m^3) (Kute et al., 2001; Lowe et al., 1980) is defined as,

$$SP = \frac{1}{A_o} \sum_{i=1}^{total\ cells} |WSSG|_i \, a_i \qquad (5)$$

The *SP* is utilized to measure the degree of haemodynamic variation along the surfaces of the LCA. High *SP* values denote high spatial flow variation.

2.4 Increasingly fine scales near the blood vessel wall

The used mesh was based on the computational results of mesh-independence studies. Meshes were created with a larger number of nodes in the radial direction. Thus, the number of nodes located in the near to the artery wall areas was significantly higher to those at vessel wall centre-line regions. Figures 1a,b show grid scale effects on molecular viscosity (kg/m-s) distribution using sparse (~135000) and dense (~620000) grid nodes, respectively. Results indicate that the sparse grid inadequately describe the molecular viscosity distribution and consequently the *WSS* in the LCA. Differences between grids appear in molecular viscosity ranges, particularly in the low molecular viscosity range (<0.0034 kg/m-s). This indicates the importance of using dense gridding near to low *WSS* flow regions (endothelium regions) and, probably, of the attraction of using a mathematically mesoscopic model such as Lattice Boltzmann.

3. Results and Discussion

Any non-zero value of the *WSSG* denotes a non-uniform haemodynamic environment. At the LMCA bifurcation region, high *WSSG* values tend to form a "ring" located at the origin of the LCxA. Further observation reveals that the distribution of *WSSG* is highly non-uniform. *WSSG* values increase in the downstream flow. Table 1 shows the I_G factor using various molecular viscosity models at the averaged inlet flow velocity magnitude of 0.17 m/s (resting conditions). Low values of I_G (<25.0%) indicate that the blood behaves as Newtonian fluid. It is the Non-Newtonian power law model that yields values of I_G greater than 25.0%. As the inlet velocity value increases, the I_G values tend to decrease (not shown).

a)

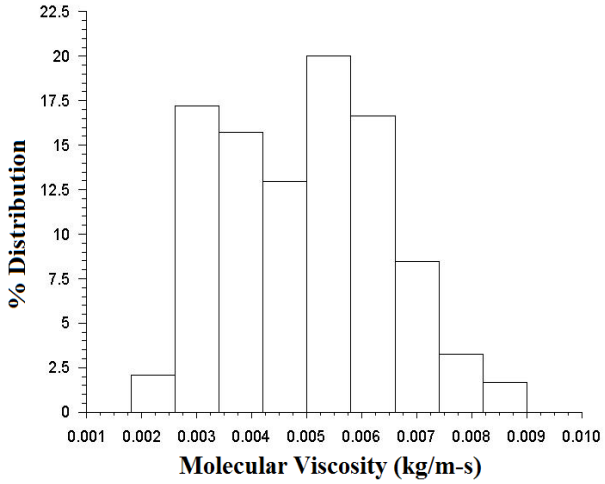

b)

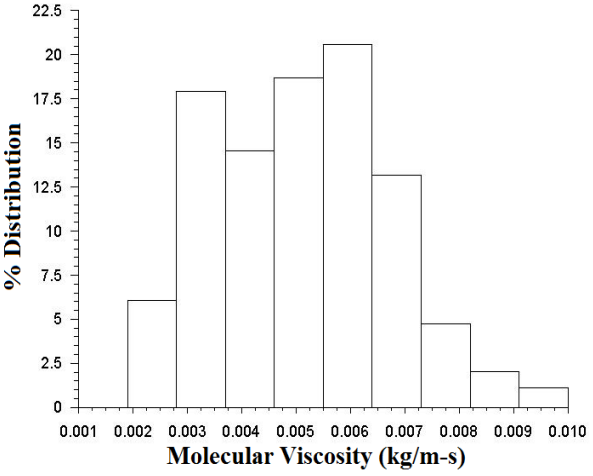

Fig. 1. Distribution of molecular viscosity (kg/m-s) for the LCA using non-Newtonian power law model, a) sparse grid and b) fine grid

Figure 2 shows the I_L factor and it refers to non-Newtonian power law molecular viscosity ratio. Non-dimensionalization is performed against Newtonian molecular viscosity value (=0.00345 kg/m-s). The I_L factor attains values

greater than 1.0 throughout the LCA. For the bifurcation shown, this value reaches 3.69 units. Patches of highly non-Newtonian behaviour are located in the concave region of the LCA bifurcation, opposite to flow divider.

Walburn-Schneck	Non-Newtonian Power Law	Generalized Power Law	Power Law
0.161	0.767	0.061	0.120

Carreau	Casson	Modified Cross
0.104	0.118	0.067

Table 1. Global non-Newtonian importance factor I_G (x100 %*)* using various models

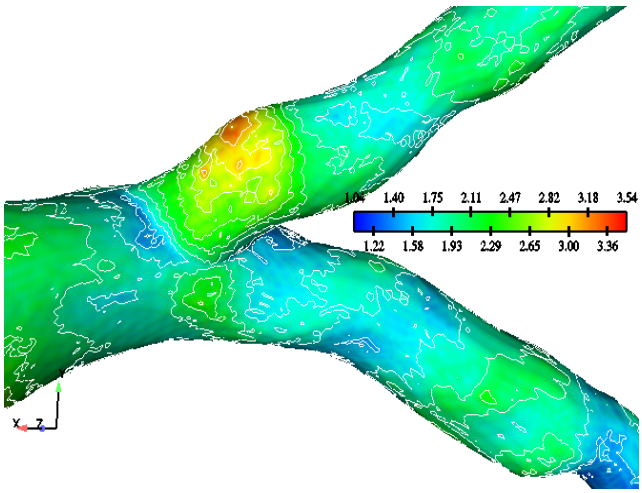

Fig. 2. Contours of local non-Newtonian importance factor I_L. The I_L factor refers to non-Newtonian power law molecular viscosity ratio. Non-dimensionalization is performed against Newtonian molecular viscosity value (=0.00345 kg/m-s)

Table 2 shows the calculated *SP* values under resting flow conditions. It is apparent that the differences in the calculated *SP* values, using different molecular viscosity models, are great. This is due to the high sensitivity of the *SP* parameter. The *SP* parameter is highly sensitive and it is a better hemodynamic factor to assess the *WSS* behaviour using various viscosity models.

Table 3 shows the calculated area averaged *WSS* (N/m^2), also at resting flow conditions. Each model has its own particular distribution, which depends upon the applied molecular viscosity formula. The non-Newtonian power law model averaged *WSS* value is 13.34 N/m^2. Power law model gives the smaller area averaged *WSS* value of 5.82 N/m^2.

Walburn-Schneck	Newton-ian	Non-Newtonian Power Law	Generalized Power Law
5024	8713	7038	8803

Power Law	Carreau	Casson	Modified Cross
2346	8786	9395	8800

Table 2. Area averaged *WSSG* (N/m^3) (*SP* parameter) using various molecular viscosity models

Walburn-Schneck	Newton-ian	Non-Newtonian Power Law	Generalized Power Law
8.88	11.92	13.34	12.04

Power Law	Carreau	Casson	Modified Cross
5.82	12.28	12.89	12.18

Table 3. Area averaged *WSS* (N/m^2) using various molecular viscosity models

For the non-Newtonian power law model, the molecular viscosity values range from 0.0044 kg/m-s to 0.0114 kg/m-s, Fig. 3a. Note that the above range is the widest one of all tested molecular viscosity models. The range between maximum and minimum molecular viscosity values using Carreau law, Modified cross law, Generalized power law model (Fig. 3b) and Casson law, for the same LCA bifurcation region, is relatively narrow (0.00345-0.0065 kg/m-s). Even narrower is the range of molecular viscosity values for the Walburn-Schneck law model (0.0024-0.0055 kg/m-s). The power law model gives molecular values ranging between 0.0006 and 0.0093 kg/m-s. In all complex patterns of molecular

viscosity distribution, using any of the non-Newtonian blood flow models, the endothelium

a)

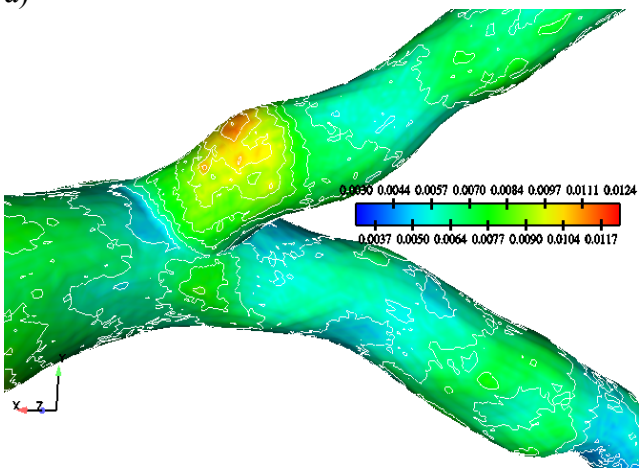

b)

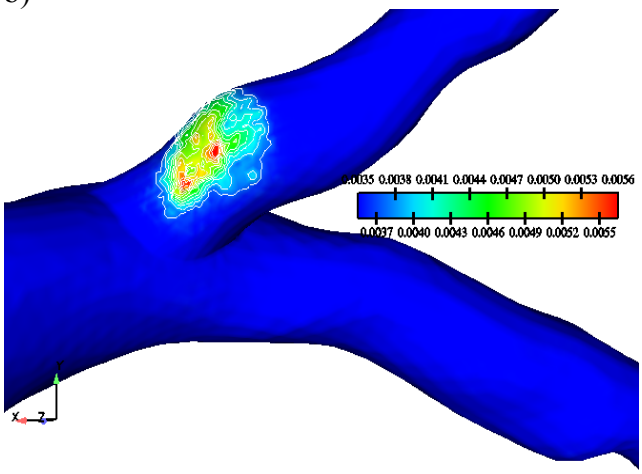

Fig. 3. Molecular viscosity μ (kg/m-s) magnitude distribution, a) Non-Newtonian power law b) Generalized power law

flow regions opposite to the flow divider at the outer walls of the major bifurcation attain high values. Low strain rates appear in these regions and the capabilities of the various blood models are clearly seen in the above figures. At high strain rates the differences in molecular viscosity values between Newtonian and non-Newtonian blood flow models are small. On the LCA bifurcation, at regions opposite to the flow divider, dominant low *WSS* values occur, Figs. 4a,b. High curvature affects the velocity distribution at the flow divider, giving rise to high *WSS* values. Note that the *WSS* values increase from proximal to distal LAD parts. This *WSS* pattern is predicted in all molecular viscosity models.

a)

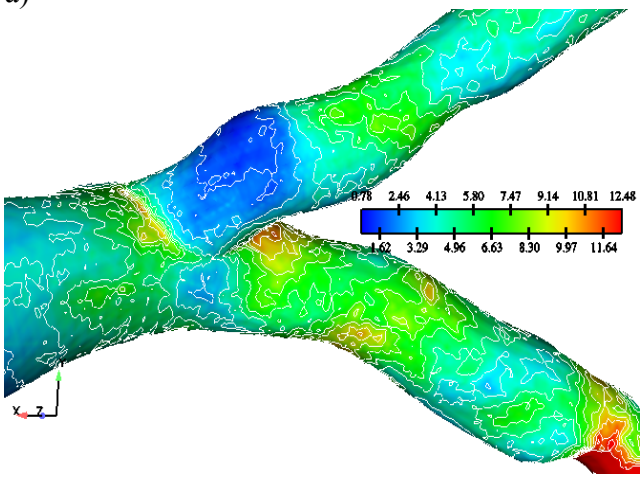

b)

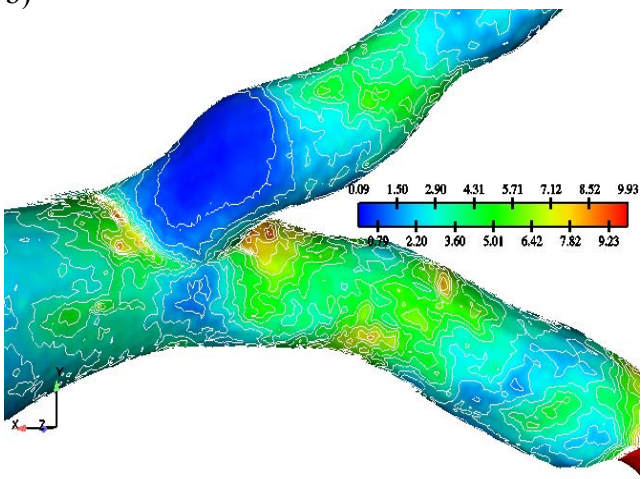

Fig. 4. *WSS* (N/m^2) magnitude distribution, a) Non-Newtonian power law, b) Generalized power law

Our results, using any of the molecular viscosity models, show that there are three distinct regions within the flow possessing high molecular viscosity values: a) The flow region, located near to centre of the cross-sectional area of any segment, is characterized by high magnitudes of velocity and occupies a large section of the lumen followed by a region of reduced molecular viscosity values extending up to the endothelium. b) High molecular viscosity values appear at proximal LCA regions. The magnitude of molecular viscosity decreases from proximal to distal flow dividers. This is due to the fact that the vessel geometry is highly tapered. Thus, the flow velocity increases from proximal to distal parts. Subsequently, the *WSS*

increases and the molecular viscosity decreases. c) Flow regions at the lateral walls opposite to the flow dividers, are regions of high molecular viscosity values. In all complex patterns of molecular viscosity distribution, using any of the non-Newtonian blood flow models, the endothelial surfaces in the regions opposite to the flow divider at the outer walls of the major bifurcation attain high values. Low strain rates appear in these regions and the capabilities of the various blood models are clearly seen in the above figures.

4. Finer scale studies

Historically, the different, essentially empirical, viscosity models used in this study originate from a range of well-accepted applications, encompassing polymer rheology, colloids, suspensions, nematic liquid crystals and, of course, blood flow: the variety is considerable, as is the physical origin of non-Newtonian behaviour- a polymer's visco-elasticity originates in the ability of its constituent macro-molecules to "unravel" and to align in an applied shear whilst, in hemodynamics, non-Newtonian behavior originates in the elastic deformation properties of the suspended, advected cells.

Given the differences in the underlying physics, it is surprising that the range of models used in this study have been so successfully applied here and elsewhere and impossible not to question if one model is best-suited to the simulation of blood flow or, at least, more well-founded. The answer to such a question is, of course, not to be found by investigating the length scales of the present study. Rather, one must consider the meso-scale dynamics of blood. Such an investigation calls for techniques, well-adapted to large numbers of Lagrangian particles, or cell. Explicit simulations of $o(10^2)$ elastically deformable erythrocytes in Newtonian plasma have been achieved using lattice Boltzmann equation method (Dupin et al., 2007) and the same essential technique, applied to high volume-fraction suspensions of mutually immiscible drops, all with Laplacian inter-facial tension has, very recently, demonstrated emergent power law behavior, (Spencer et al. 2011. Clearly, it is possible that, combined with appropriate experimental measurements, such micro-scale investigations of modalities unresolved by mainstream, continuum hemodynamics may reduce uncertainties and degeneracy in studies such as that we report here.

5. Conclusions

Results derived from any of the applied non-Newtonian law model indicate that patches of highly non-Newtonian behavior are located in the concave region of the LCA bifurcation, opposite to flow divider. The *WSS* distribution yields a consistent LCA tree pattern for nearly all non-Newtonian models. The global importance factor for the non-Newtonian law model yields 76.7% (non-Newtonian flow), while for the Generalized power law model this value is 6.1% (Newtonian flow). High molecular viscosity and low *WSS* and *WSSG* values appear at proximal LCA regions at the outer walls of the major bifurcation. High *SP* values denote high spatial flow variation. The Non-Newtonian power law, Generalized power law, Carreau and Casson and Modified cross blood viscosity models give comparable molecular viscosity, *WSS* and *WSSG* values. The Newtonian blood flow treatment is considered to be a good approximation at mid and high strain rates. The capabilities of the applied non-Newtonian law models appear at low strain rates. In general, the non-Newtonian power law and the Generalized power law blood viscosity models are considered to approximate the molecular viscosity and *WSS* calculations in a more satisfactory way.

References

Abraham, F., Behr, M., Heinkenschloss, M., 2005. Shape optimization in unsteady blood flow: A numerical study of non-Newtonian effects, Comput. Methods Biomech. Biomed. Engin., 8(3), 201-212.

Ballyk, P.D., Steinman, D.A., Ethier, C.R.,1994. Simulation of non-Newtonian blood flow in an end-to-side anastomosis. Biorheology, 31, 565-586.

Becker, R.C., 1993. The role of blood viscosity

in the development and progression of coronary artery disease. Cleve. Clin. J. Med., 60, 353-358.

Cho, Y.I., Kensey, K.R., 1991. Effects of the non-Newtonian viscosity of blood on flows in a diseased arterial vessel, Part 1: Steady flows. Biorheology, 28, 241-262.

Coskun, A.U., Yeghiazarians, Y., Kinlay, S., Clark, M.E., Ilegbusi, O.J., Wahle, O., Sonka, M., Popma, J.J., Kuntz, R.E, Feldman, C.L., Stone, P.H., 2003. Reproducibility of coronary lumen, plaque, and vessel wall reconstruction and of endothelial shear stress measurements in vivo in humans. Catheter Cardiovasc. Interv. 60, 67-78.

Dupin, M.M., Halliday,I., Care, C.M., Alboul, L., Munn, L.L, 2007. Modeling the flow of dense suspensions of deformable particles in three dimensions. Phys. Rev. E 75, 066707.

Farmakis, T.M., Soulis, J.V., Giannoglou, G.D., Zioupos, G.J., Louridas, G.E., 2004. Wall shear stress gradient topography in the normal left coronary arterial tree: possible implications for atherogenesis. Curr. Med. Res. Opin., 20, 587-596.

Fung, Y.C., 1976. Biomechanics: Mechanical properties of living tissues. 2nd Edition Springer, Berlin 571 pp.

Ghista, D.N., Van Vollenhoven, E., Yang, W.-J., Reul, H., 1979. Blood: Rheology, hemolysis, gas and surface interactions. S. Karger, New York. 165 pp.

Giannoglou, G.D., Soulis, J.V., Farmakis, T.M., Giannakoulas, G.A., Parcharidis, G.E., Louridas, G.E., 2005. Wall pressure gradient in normal left coronary artery tree. Medical Engineering and Physics, 27(6), 455-464.

Johnston, B.M., Johnston, P.R., Corney, S., 2004. Non-Newtonian blood flow in human right coronary arteries: steady state simulations. J. Biomech., 37, 709-720.

Junker, R., Heinrich, J., Ulbrich, H., Schonfeld, R., Kohler, E., Assman G., 1998. Relationship between plasma viscosity and the severity of coronary heart disease. Arterioscler. Thromb. Vasc. Biol., 18, 870-875.

Kute, S.M., Vorp, D.A., 2001. The effect of proximal artery flow on the haemodynamics at the distal anastomosis of a vascular bypass graft: computational study. J. Biomech. Eng., 123(3), 277-283.

Lei, M., Giddens, D.P., Jones, S.A., Loth, F., Bassiouny, H., 2001. Pulsatile flow in an end-to-side vascular graft model: comparison of computations with experimental data. J. Biomech. Eng., 123, 80-87.

Lowe, G.D., Drummond, M.M., Lorimer, A.R., Hutton, I., Forbes, C.D., Prentice, C.R., Barbenel, J.C., 1955. Relation between extent of coronary artery disease and blood viscosity. Br. Med. J., 280, 673-674.

Murray, C.D., 1926. The physiological principle of minimum work. I. The vascular system and the cost of blood volume. Proc. Natl. Acad. Sci., 12, 207–214.

Sharma, K., Bhat, S.V., 1992. Non-Newtonian rheology of leukemic blood and plasma: are n and k parameters of power Law model diagnostic? Physiol. Chem. Phys. Med. NMR, 24, 307-312.

Soulis, J.V., Farmakis, T.M., Giannoglou, G.D., Hatzizisis, I.S., Giannakoulas, G.A., Parcharidis, G.E., Louridas, G.E., 2006. Molecular viscosity in the normal left coronary arterial tree. Is it related to atherosclerosis? Angiology, 57(1), 33-40.

Spencer, T.J., Halliday, I., Care, A.M., 2011. A local lattice Boltzmann method for multiple immiscible fluids and dense suspensions of drops. Phil. Trans. R. Soc. A 13, 369(1944), 2255-2263.

Walburn, F.J., Schneck, D.J., 1976. A constitutive equation for whole human blood. Biorheology, 13(3), 201-210.